# Supplementary Information: Highly sensitive detection of physiological spins in a microfluidic device

*Florestan C. Ziem, Nicolas S. Götz, Andrea Zappe, Steffen Steinert, Jörg Wrachtrup*

3rd Institute of Physics and Research Center SCOPE,

University Stuttgart, Stuttgart 70569, Germany

**NV relaxation rate**

In the main text, sensing of paramagnetic species via observation of the longitudinal relaxation rate $\Gamma_1 = 1/T_1$ of the nitrogen-vacancy centers (NVs) is described. $\Gamma_1$ is the integrated product of the normalized resonance line of the spin transition with the power spectrum of the spin noise. The response of the NV spin can be treated as a d-function in frequency, such that at vanishing magnetic field, $\Gamma_1$ is given by two times the power spectrum at the zero-field splitting frequency $D$, where the factor 2 takes into account both transitions from $m_s = 0$ to $m_s = \pm 1$. As given in the main text, this results in

$$\Gamma_1 = \frac{2\langle B^2 \rangle f_t}{f_t^2 + D^2} \quad \text{(Supplementary Eq. 1).}$$

where $\langle B^2 \rangle$ in terms of frequency is the mean square interaction strength between the external spin bath and the $x$- and $y$-component of an NV. $f_t = f_{int} + f_{dip} + f_{rot} + f_{dif}$ is the composite relaxation rate of the external spins. Contributions $f_{int}$ are usually in the MHz to GHz range and stem from hyperfine shifts due to the immediate environment[1,2]. Rotation adds fluctuations within the same range, as determined from Stokes law and strongly depends on the size of the complex. Spatial diffusion accounts for about 40 MHz, as determined from the temporal autocorrelation of the dipolar interaction between an NV and a passing ion.[3] Assuming a constant mutual relaxivity $r_{dip}$ between the diffusing spins, such that $f_{dip} = r_{dip} \times n$, and substituting $f_t$ into Supplementary Equation (1), the proportionality of $\Gamma_1$ to $1/r_{dip}$ can be obtained.

**Interaction strength for homogeneous spin distributions**

When single paramagnetic ions are homogeneously distributed within the volume above the NV ensemble sensor, the mean interaction between the external spin bath and an NV can be obtained by integrating the square interaction strength times the constant ion density over the volume. One obtains[3]

$$\left\langle B^2 \right\rangle = \left( \frac{\mu_0}{4\pi\hbar} g_{\mathrm{NV}} g_{\mathrm{S}} \mu_{\mathrm{B}}^2 \right)^2 \frac{n\pi(z^3 - d^3)}{16 z^3 d^3} \left( S(S+1) + \frac{1}{2S+1} \sum_{m=-S}^{S} m^2 \right) \qquad \text{(Supplementary Eq. 2),}$$

where $g_{NV}$ and $g_S$ are the g-factors of the NV and the external spins, respectively, $n$ is the number density of the external spins and $S$ their spin quantum number. $d$ is the depth of the NVs below the diamond surface and $z$ is the upper integration limit when considering a finite layer of the solution, i.e. ($z$ - $d$) is the layer thickness. This formula applies to the manganese ions in the main text.

**Relaxation rate due to a monolayer of adsorbed manganese(II)**

To model the relaxation rate of manganese(II) adsorbed in a monolayer on the diamond surface, we used Supplementary Eq. 1 and 2, and took the sum of the diameter of the $Mn^{2+}$ ion and one of the coordinated water molecules (0.29 nm) [4] as the layer thickness. As described in context of Figure 2a in the main text, above a concentration of 0.2 mol/l the dependence of the relaxation rate on concentration is dominated by freely diffusing ions. We took this concentration as the effective concentration in the adsorption layer and did not take contributions of rotation and diffusion to the manganese spin fluctuation rate into account. The mutual relaxivity, $r_{\mathrm{dip}}$ = 6 GHz/mol, was obtained from the behavior above 0.2 mol/l concentrations, as explained in the main text.

**Interaction strength for clustered spins**

In case of ferritin, a homogeneous distribution of the external spins is not the case and almost all contribution to the NV relaxation stems from the nearest neighbor molecule in the concentration range applied in our experiments. The probability density function of finding the $i$-th next neighbor molecule to a given NV at distance $r \geq d$ is given by[5,6]

$$w_{n,i}(r) = \frac{n^i V' V^{i-1}}{(i-1)!} \exp(-nV).$$

*d* is the depth of the NV below the diamond surface, *n* is the number density of ferritin, given here in either three or two dimensions. $V = V_d(r)$ is, in our case, the volume given by the intersection of a sphere of radius *r* around the NV and the volume in which the particles are distributed, where *d* enters as a constant parameter. In three dimensions (particles in solution) this intersection is a spherical cap and a circle in two dimensions (adsorbed particles). *V'* is the derivative of *V* with respect to *r* in three dimensions and with respect to the diameter of the circle (the projection of r onto the diamond surface) in two dimensions.

To calculate the relaxation rate, we treated the ferritin core as paramagnetic and employed its magnetic moment due to statistical polarization, i.e. proportional to the square root of the number of spins within a ferritin core. We weighted the square interaction strength $B_{xy}(r)^2$ between this effective magnetic moment and the *x*- and *y*-component of the NV, with the probability density $w_{n,i}(r)$ and integrated over *r* to obtain the mean NV relaxation rate for a given concentration. The results of these calculations are shown in Supplementary Figure 1. At the maximum concentrations applied in our experiments, the probability density function of the nearest neighbor peaks at ~45 nm and ~25 nm in the solution and adsorption cases, respectively. While the higher order neighbors can be expected to be found just several nanometers further away, the $r^{-3}$ dependence of the dipole-dipole coupling results in negligible contributions within our concentration range.

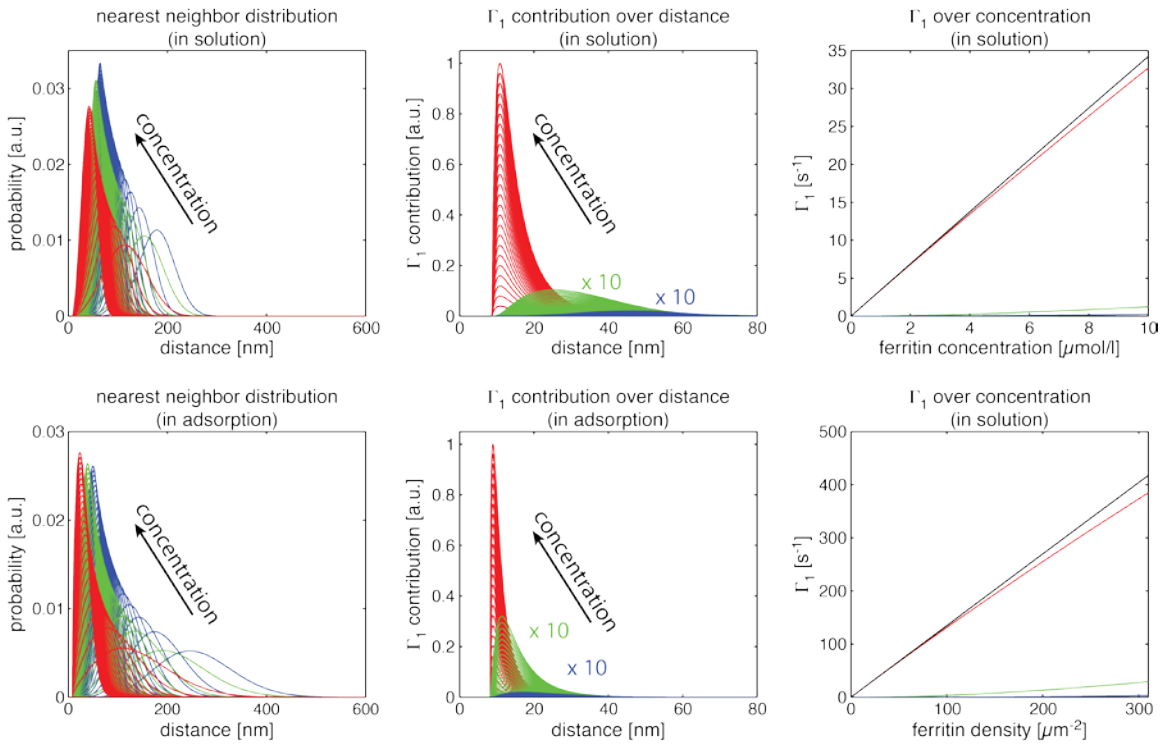


**Supplementary Figure 1** Nearest neighbor distributions and resulting relaxation for ferritin in solution (upper row of graphs) and in adsorption (lower row). The first graph in each row shows the probability density function of the distance of the next (red), 2nd next (green) and 3rd next neighbor (blue) for the concentration range applied in our experiments. Each line of the same color represents one concentration. The second graph in each row shows the contributions to relaxation, weighted by the probability density function $w_{n,i}(r)$. Contributions of 2nd (green) and 3rd (blue) next neighbor have been scaled by a factor of 10. The third graph shows the resulting relaxation rates, dominated by the contribution of the nearest neighbor (red). The black curve is the sum of the contributions of the three nearest neighbors.

**Number of adsorbed ferritin molecules versus applied concentration in solution**

After preparing adsorbed ferritin molecules on the diamond (Methods section in the main text) and measuring $T_1$, we scanned the diamond surface with an atomic force microscope and extracted the number densities of the adsorbed ferritin molecules. Supplementary Figure 2 shows a scatter plot of the ferritin number density vs. the applied concentration. To obtain an approximate conversion factor from concentration in solution to number density in adsorption, we applied a linear fit to the data and through the origin, which yielded a $(31.6 \pm 3.3)$ $\mu m^{-2}/(\mu M)$.

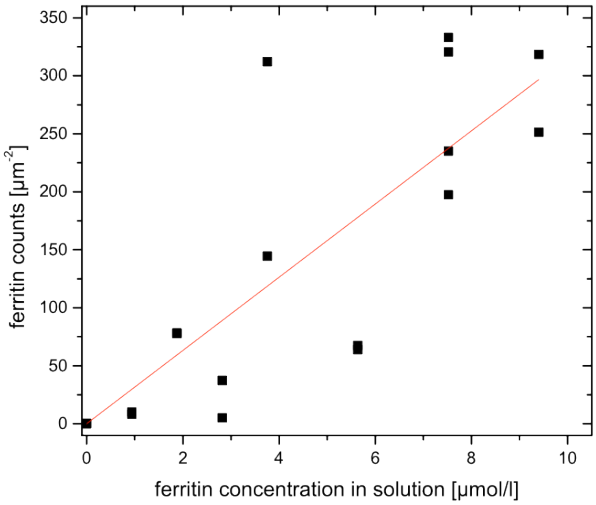


**Supplementary Figure 2** Adsorbed ferritin number densities after exposing the diamond surface to ferritin solutions of several concentrations. The red line is a linear fit to the data and through the origin with slope 32 $\mu m^{-2}/(\mu M)$.

**Manganese adsorption dynamics and 'filling offset' in ferritin measurements in the flow cell**

Figures 2b and 2c show single-τ measurement performed at flow rates of ~5 µl/s, where the channel diameter is approximately 100 µm. Upon reduction of the flow rate, less ions are introduced at a time, and a steady state of adsorption is reached on longer time scales. This behavior is shown in Supplementary Figure 3, where a 100 nmol/l solution of $MnCl_2 \cdot 4H_2O$ was introduced at a flow rate of 0.75 µl/s. We expect similar behavior upon introduction of ferritin in the flow cell, but attempts to measure single-τ curves with ferritin resulted in fluctuations of the signal, without reaching a steady state. Before the full $T_1$ measurements of ferritin in solution were performed, several hundred µl of the solution passed through the flow cell at rate of several µl/s and then the flow was stopped. During this filling phase, we presume that excess molecules were deposited on the diamond surface, leading to the offset in relaxation rate observed in Figure 3b in the main text.

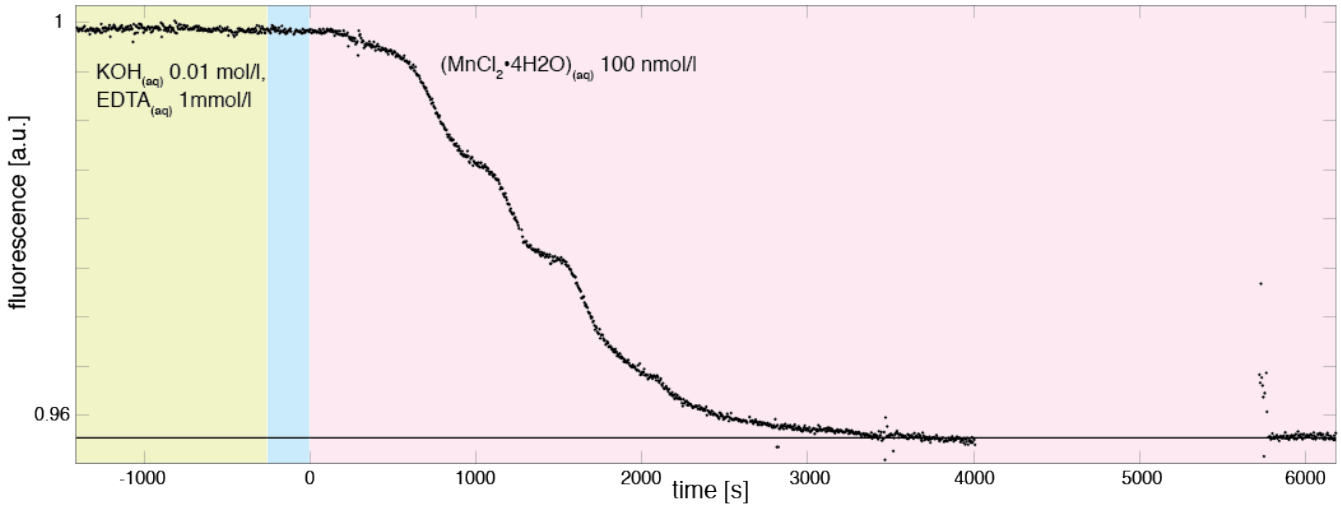


**Supplementary Figure 3** Single-τ measurement showing the introduction of a manganese(II) solution with concentration 100 nmol/l into the flow cell. At a low flow rate, the steady adsorption of ions on the diamond surface could be witnessed, until a steady state was reached. The initial fluorescence level corresponds to a clensing solution of potassium hydroxide and ethylenediaminetetraacetic acid (EDTA) followed by a buffer of Milli-Q (Millipore, Bedford, MA) water to separate it from the manganese solution.

**Supplementary references**

(1) Kruk, D.; Kowalewski, J.; Westlund, P.-O. *The Journal of chemical physics* **2004**, *121*, 2215–27.
(2) Sur, S. K.; Bryant, R. G. *The Journal of Physical Chemistry* **1995**, *99*, 6301–6308.
(3) Steinert, S.; Ziem, F.; Hall, L. T.; Zappe, A.; Schweikert, M.; Götz, N.; Aird, A.; Balasubramanian, G.; Hollenberg, L.; Wrachtrup, J. *Nature Communications* **2013**, *4*, 1607.
(4) Marcus, Y. *Chemical Reviews* **1988**, *88*, 1475–1498.
(5) Hertz, P. *Mathematische Annalen* **1909**, *67*, 387–398.
(6) Berberan Santos, M. *American Journal of Physics* **1987**, *55*, 952.